Fracture behavior of the concrete cover due to rebar corrosion

Y. Kitsutaka
Tokyo Metropolitan University, Tokyo, Japan

K. Arai
Taisei Construction Co., Tokyo, Japan

ABSTRACT: Evaluation of the performance recovery of reinforced concrete (RC) members by repair is an important issue in recent years. In this paper, first, fracture behavior of concrete RC cover with cracks due to the rebar corrosion was analyzed by using fracture mechanics approach and the diagrams to evaluating the degree of rebar corrosion by a concrete surface crack width and rebar diameter were proposed. Next, effects of the repairing material properties of polymer cement mortar (PCM) on fracture properties of RC cover were evaluated by a bending test of center notched small cubic RC specimen. Strength recovery by repairing is satisfactory regardless of the rebar corrosion. Toughness is also significantly improved by the repairing. The degree of improvement to toughness becomes greater as the volumetric content of fibers of PCM.

1 INTRODUCTION

Extending the service lives of buildings has become increasingly important from the standpoint of global environmental protection and economic efficiency. Maintenance of reinforced concrete buildings, which are in stock in large quantities, is particularly of social significance. In order to improve the durability of reinforced concrete structures, it is essential to select a repair method suitable for the identified deterioration phenomena of existing structures. Deterioration phenomena critical to reinforced concrete structures are interpreted as reductions in the reinforcement strength causing reductions in the structural capacity of members due to reinforcing steel corrosion, which is aggravated by cracking in cover concrete under expansive and tensile stresses resulting from reinforcement corrosion and/or aggregate reaction. In other words, it is vital for the durability of concrete that the concrete be sound and resistant to expansive and tensile forces causing cracking and that the cover including reinforcement develop sufficient strength performances. To this end, it is important to be able to evaluate the strength of cover concrete for reinforcement when deteriorative actions have caused corrosion on reinforcement and reduced its adhesion. It is also crucial to be able to evaluate the strength restoration of such cover concrete after repair and estimate the degree of reinforcement deterioration. Nevertheless, few studies have dealt with these subjects.

In this study, a method of estimating the amount of reinforcement corrosion from the crack width on the surfaces is proposed based on fracture mechanics approach. Also the authors investigated methods of evaluating the fracture properties of cover concrete including reinforcement and experimentally examined the effects of the degree of reinforcement corrosion and the repair methods on such fracture properties.

2 ESTIMATION OF THE DEGREE OF CORROSION FROM SURFACE CRACK WIDTH

2.1 *Analysis method*

The changes in the surface crack width due to reinforcement corrosion were estimated by nonlinear analysis using techniques used in fracture mechanics. The CMOD under mode I (tensile) deformation due to reinforcement corrosion was modeled by applying stresses perpendicular to the crack surfaces (mode l). Two models representing before and after the crack reached the surface were formulated as shown in Figure 1 (a) and (b).

Crack propagation is modeled by means of the fictitious crack concept with cohesive forces. The relationship of expansion load and displacement is obtained by solving the equilibrium equations for stress intensity factors, the crack opening displacement (COD) at the crack surface, and constitutive function of cohesive stress and COD. These equations are as follows:

$$K(a) = K_p(a) + K_r(a) \tag{1}$$

$$\delta(a,x) = \delta_p(a,x) + \delta_r(a,x) \tag{2}$$

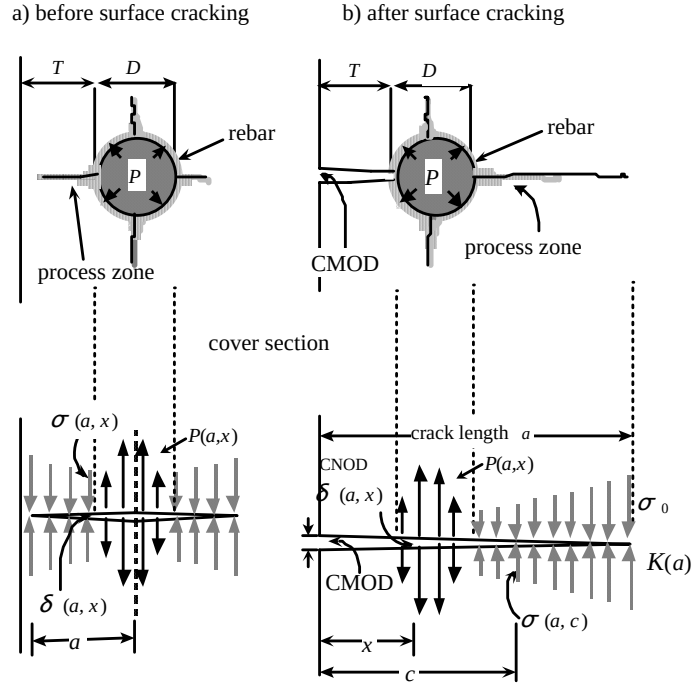

Figure 1. Models of cracking due to rebar corrosion

where, a is the crack length, x is the point on crack surface in which the COD is calculated, $K(a)$ is the total stress intensity factor on crack tip, $K_p(a)$ is the stress intensity factor due to rebar expansion load, K_r(a) is the stress intensity factor due to cohesive stress, $\delta(a,x)$ is the COD on x, $\delta_p(a,x)$ is the COD on x due to rebar expansion load, $\delta_r(a,x)$ is the COD on x due to cohesive stress and $\sigma(a,x)$ is the cohesive stress on x.

Expansion stress due to rebar corrosion $P(a, x)$ is modeled by assuming the pressure on the rebar surface is uniform as $P_0(a)$ and acting only the crack opening direction.

$$P(a,x) = P_0(a) \cdot I(x);$$
$$I(x) = \sqrt{1-\left(1-\frac{2(x-T)}{D}\right)^2}, \quad (T \le x \le T+D) \tag{3}$$

where, T is the concrete cover, D is the rebar diameter, $I(x)$ is the function of stress component.

The relationship between $\delta(a,x)$ and $\sigma(a,x)$ shown in Figure 1 is the tension softening diagram considered a material property. Applying the bi-linear approximation for a tension softening diagram, we obtain

$$\sigma(a,x) = m(\delta,x) \cdot \delta + n(\delta,x);$$
$$\delta = \delta(a,x), \tag{4}$$
$$m(\delta,x) = \begin{cases} m_1 = (f_t - \sigma_1)/\delta_1, & (0 < \delta \le \delta_1) \\ m_2 = \sigma_1/(w_c - \delta_1), & (\delta_1 < \delta \le w_c) \end{cases}$$

where, $m(\delta,x)$ and $n(\delta,x)$ are coefficients of a linear simple equation of multilinear softening curve, δ is COD, σ is the cohesive stress, and w_c is the critical value of COD.

The stress intensity factor in the Figure 1. (a) and (b) cases by mode I stresses on crack surface are given by (Tada 1985)

$$K_I = \frac{2f}{\sqrt{2d}} G(a,c,d), \; K_I = \frac{2f}{\sqrt{\pi a}} G(a,c,d) \tag{5}$$

where, f is node force, d is the width of the body, c is the co-ordinate indicating the point on crack surface where cohesive stress is acting, and $G(a,c,d)$ is the weight functions (APPENDIX).

So stress intensity factors in Equation (2) are normalized as

$$K_p(a) = P(a) \int_0^a I(c) g_1(a,c) dc \tag{6}$$

$$K_r(a) = \int_0^a \sigma(a,c) g_1(a,c) dc \tag{7}$$

Castigliano's theorem can be applied for the calculation of COD for uniform materials. Displacement of the cracked body can be expressed as

$$d\delta = \delta_0 + \frac{2}{E} \int_x^a K(z) \left[\frac{\partial K_F(z)}{\partial F} \right]_{F=0} dz \tag{8}$$

where, dy is the displacement, d_0 is the displacement of the uncracked body, z is the co-ordinate indicating the crack length for the integration, f is the fictitious force acting on the point z, $E^*(z)$ is the generalized equivalent elastic modulus of the material on z (i.e., E for plane stress, and $E/(1-\nu 2)$ for plane strain, where E and n is Young's modulus and Poisson's ratio respectively), and $K_f(z)$ is the stress intensity factor due to fictitious force f. From (7), crack opening displacements, $\delta_p(a,x)$ and $\delta_r(a,x)$ can be obtained as

$$\delta_p(a,x) = \frac{P(a)}{E} \int_0^a I(c) g_2(a,x,c) dc \tag{9}$$

$$\delta_r(a,x) = \frac{1}{E} \int_0^a \sigma(a,c) g_2(a,x,c) dc \tag{10}$$

Substituting (6) and (7) into (1), also (9) and (10) into (2), and with cancellation of $P(a)$, the fundamental simple crack integral equation is obtained (Kitsutaka 1997) as

$$\delta(a,x) = \frac{1}{E} \int_0^a \sigma(a,c) H^e(a,x,c) dc;$$
$$H^e(a,x,c) = g_2(a,x,c) - g_1(a,c) \frac{\int_0^a I(c) g_2(a,x,c) dc}{\int_0^a I(c) g_1(a,c) dc} \tag{11}$$

where, $H^e(a,x,c)$ is the weight function (called as H-function) of the specimen and does not depend on the external forces and the cohesive stresses.

Substituting $\sigma(a,x)$ of (4) into the crack integral equation of (11) and expressing in the matrix form for the total number of nodes (=n) on the crack surface, we get the simultaneous crack equations. COD

of each nodes are calculated linearly by these equations. This problem can be solved by several iterations (Kitsutaka 1997). From the solution of COD, $\sigma(a,x)$ is calculated from (4). Then, $P(a,x)$ are calculated from (3).

The advantage of this analysis method is that the singular solution of COD distribution can be calculated directly by using the simultaneous crack equations with boundary conditions of H-function. Because of this singularity, we do not need to assume the crack surface profile, and the relationship between COD and the expansion stress with different types of constitutive law on each point of crack surface can be obtained by only iterating on the inclination of tension softening curves.

2.2 *Analysis results*

Figure 3 shows the analysis results related to the results of accelerated corrosion tests on specimens other than those described in the previous paper (Kitsutaka 1998). Figure 2 sows the outline of accelerated corrosion test. The tests were conducted on five mortars/concrete: normal strength plain mortar (NPL, Fc=55MPa), normal strength fiber-reinforced mortar (NVF, Fc=58MPa, Vinylon-Fiber 1%), high strength plain mortar (HPL, Fc=120MPa), high strength fiber-reinforced mortar (HVF, Fc=120MPa, Vinylon-Fiber 1%) and normal concrete (Ncon, Fc=55Mpa). Two levels of cover depths, 5 and 15 mm, were selected for reinforcing bars 10 mm in diameter. The tension softening curve for each specimen was estimated in a bilinear form. The corrosion

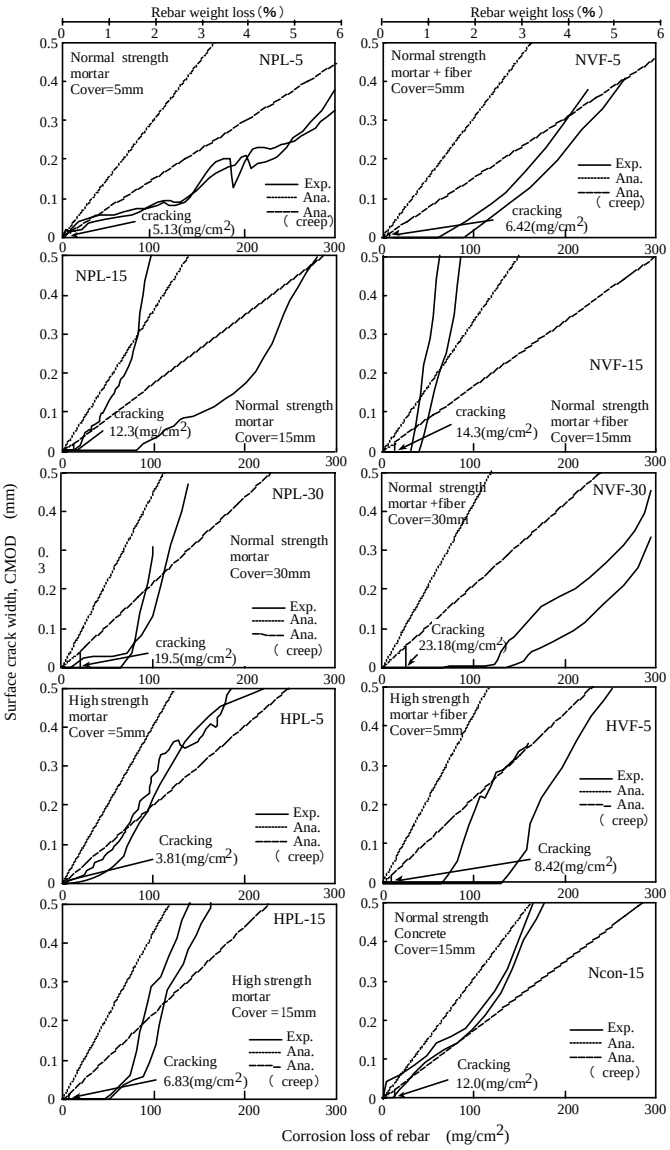

Figure 3. Results of corrosion accelerated test

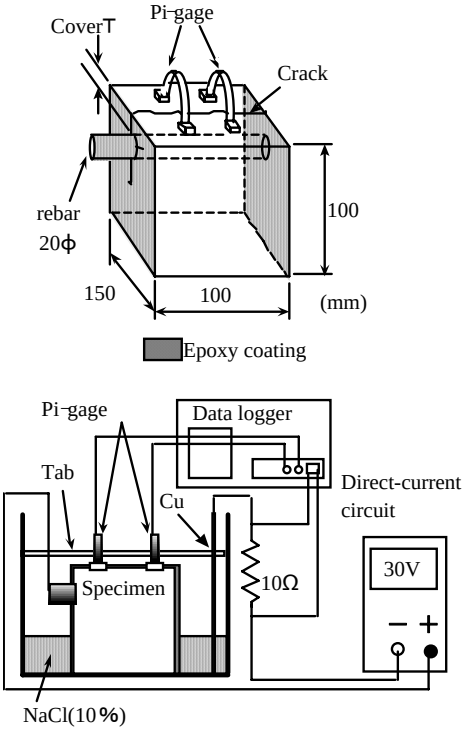

Figure 2. Outline of corrosion accelerated test

loss was calculated from the analysis results of rebar expansion (CMOD of rebar areas in the adhesion model). The elastic modulus and volumetric expansion coefficient of rust were assumed to be 250 MPa and 2.5, respectively, referring to the literature, such as reference (Kitsutaka 1998). Analysis was also conducted considering the creep deformation of concrete near the rebar. In this case, the CMOD of the rebar area for the same expansive pressure was calculated in consideration of the creep coefficient. The creep coefficients were assumed to be 1.0 and 0.5 for series N and H, respectively. Figure 3 reveals that the analysis results incorporating creep generally agree better with the test results, presumably because the plastic deformation near the rebar under expansive pressure can be expressed by the creep coefficient. Also, the analysis results of the high strength series agree better with the test results than those of the normal strength series. Whereas cracking in normal strength concrete is apt to disperse

around rebars, that of high strength concrete tends to occur singly in a brittle manner. This may be the reason for the good agreement with the adherence model, which assumes a single crack.

Figure 4 shows the relationship between the crack width and section loss ratio under various conditions based on the present analysis. The compressive strength is in three levels: 20, 50, and 100 MPa, each

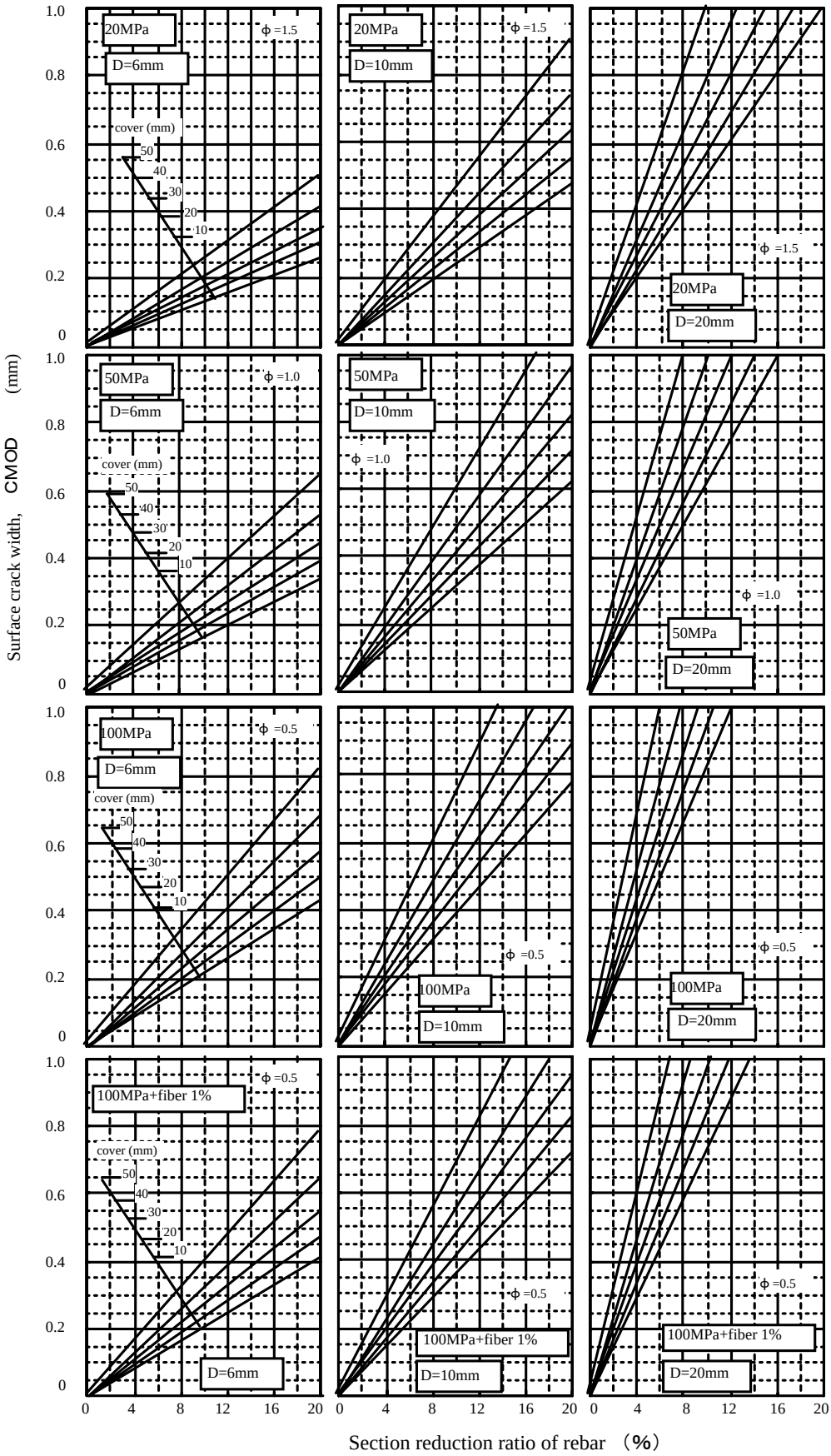

Figure 4. Relationship between the crack width and section loss ratio under various conditions

with a creep coefficient (ϕ) of 1.5, 1.0, and 0.5. The rebar diameter is in three levels: 6, 10, and 20 mm, and the cover thickness is in five levels: 10, 20, 30, 40, and 50 mm. An approximate section loss ratio of reinforcement can be estimated from the surface crack width using this diagram by selecting the concrete strength, rebar diameter, and cover depth. The section loss ratio of reinforcement increases as the crack width increases. When the crack width is the same, the section loss ratio decreases as the cover depth increases and as the bar diameter increases.

3 EVALUATION OF FRACTURE PROPERTIES OF COVER REPAIRED CONCRETE

3.1 *Test procedure*

Geometry of the specimen is same as the one showed in Figure 2. A single reinforcing bar (SD295A-D10) was placed in each prismatic specimen measuring 100 by 100 by 100 mm with a cover depth of 10 mm, assuming an insufficient cover in a reinforced concrete structure, and subjected to electrical charges to accelerate its corrosion. The protruding ends of the bar were sealed with epoxy to prevent water seepage during electrical corrosion.

The method of accelerating reinforcement corrosion is same as the method showed in Figure 2. Each specimen was immersed in a 3% NaCl solution and subjected to an electrical current from a stabilized power source through the rebar serving as the anode and copper foil serving as the cathode. This caused both anodic reaction, in which ferrous ions were dissolved while generating electrons, and cathodic reaction, in which the generated electrons were consumed for reduction of dissolved oxygen, simultaneously on the reinforcement surfaces, thereby accelerating corrosion. The cumulative amperage was continuously monitored using dataloggers, based on which the section loss ratio of reinforcement due to corrosion was changed. The relationship between the corrosion loss and the cumulative amperage was determined beforehand by conducting preliminary tests.A portable rebar corrosion meter was used to grasp the relationship between the degree of reinforcement corrosion and the half-cell potential during accelerated testing.

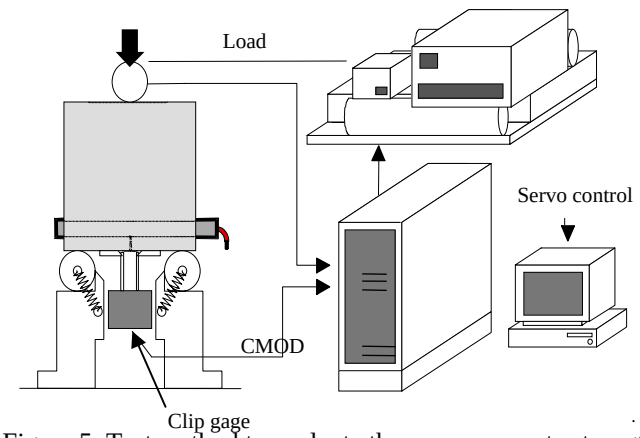

Figure 5. Test method to evaluate the cover concrete strength

3.2 *Evaluation of fracture properties of cover concrete*

A slab having corroded lowermost bars under normal loading subjected to partial flexural and shear forces was specifically assumed for this study, in order to evaluate the fracture properties of cover concrete for reinforcement. In other words, short-span three-point loading tests were conducted on the prismatic specimens to apply both bending and shear forces, with the axis being the direction of reinforcement as shown in Figure 5. Also, a notch to a depth of 10 mm perpendicular to the bar was made in the tension edge to pinpoint the location of fracture. A closed-loop servo-control hydraulic testing machine manufactured by MTS Systems Corporation was used for the tests, with the load being controlled by the crack mouth opening displacement (CMOD) at the notch. Sensitive clip gauges were used for measuring the CMOD. The load point displacements were also measured using two displacement transducers attached to the sides of each specimen.

3.3 *Test conditions*

Four concrete mixtures were proportioned: normal strength with and without fibers and high strength with and without fibers. Normal portland cement and crushed sand of hard sandstone from Tama were used as the cement and fine aggregate, respectively. The chemical admixture was an air-entraining and high-range water-reducing admixture of a polycarboxylic ether type. The fibers and reinforcement were polyvinyl alcohol (PVA) fibers 400 μm in diameter and 12 mm in length and deformed bars SD295A-D10, respectively. The factors and levels of experiment were as follows: two levels of water-cement ratios (W/Cs) (30% with the chemical admixture and 60%), two levels of fiber content (0% and 2%), and five levels of section loss ratios of rebars in specimens by electrical corrosion (0%, 5%, 10%, 15%, and 30%). These levels totalled 20.

3.4 *Repair methods and conditions*

Specimens with section loss ratios of 0%, 5%, 10%, 15%, and 30% were prepared by accelerating corrosion deterioration, to which two types of repair, patching and crack injection, were applied. Repaired specimens were further subjected to accelerated corrosion to final section loss ratios of 0%, 5%, 10%, 15%, and 30%. For patching, a polymer cement patch material made by mixing a premixed powder

comprising fibers and cement and a liquid containing polymer was used. After chipping off the deteriorated area with an impact hammer to form a V-shaped groove of a right triangular cross section, rust and concrete on rebar surfaces were removed using a wire brush, and the patch material was filled in the groove. For crack injection, a two-liquid low-viscosity acrylic crack injection compound was used. It is a product designed to retain its reactivity even when applied to cracking where water is present. After diking the area along the cracking above the rebar using a silicone sealant, 6 ml of the injection compound was allowed to seep into the cracking using a dropper. The excess compound on the concrete surface was removed after confirming the hardening of the compound.

3.5 *Test results and discussion*

From the results of compression and tension tests on concrete standard-cured for four weeks in water at 20°C. The compressive strength increases as the W/C decreases (80Mpa and 40MPa) but a little bit decreases when fibers are included. Fibers are expected to resist cracking induced by corrosive expansion pressure and cover concrete deterioration.

The section loss ratio of rebars were calculated from the cumulative amperage on the horizontal axis and the half-cell potential on the vertical axis. This reveals that the half-cell potential is in a stable state (E < -200 mV) with no corrosion (0%) in all mixtures. With a section loss ratio of 5% to 15%, the half-cell potential is plotted in both the uncertain (-200 mV ≤ E ≤ 350 mV) and corrosion (-350 mV < E) regions, whereas nearly all plots fall in the corrosion region when the section loss ratio is 30%.

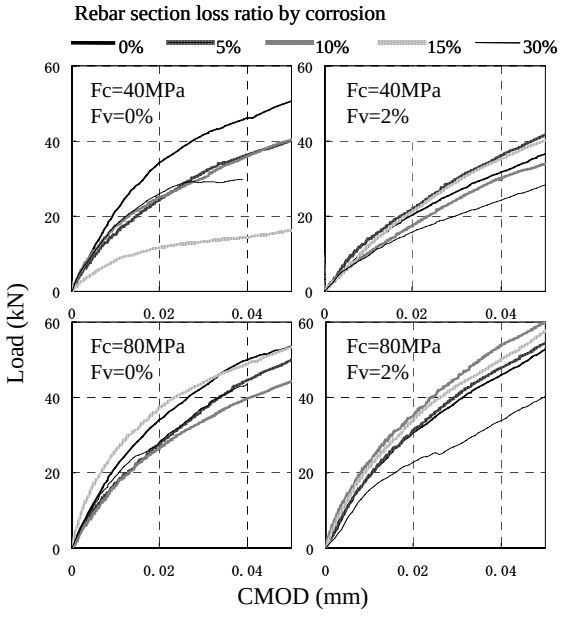

Figure 6. Results of three-point loading tests with different degrees of deterioration before repairing

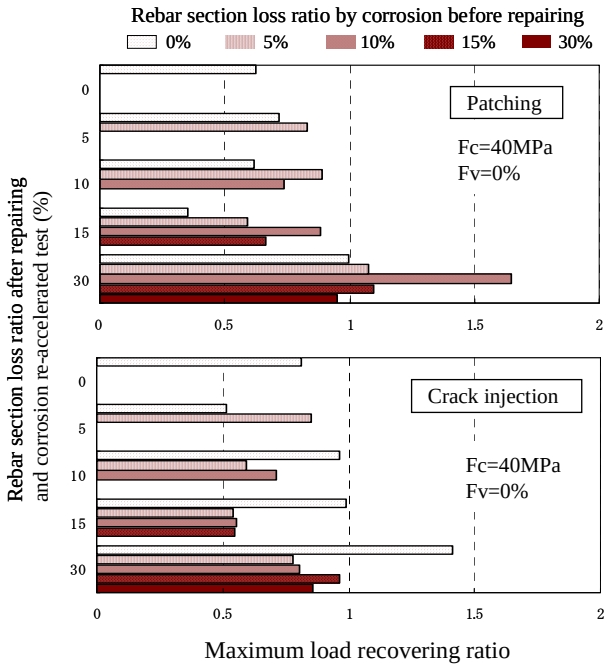

Figure 7. Maximum loads on repaired specimens and specimens subjected to accelerated rebar corrosion

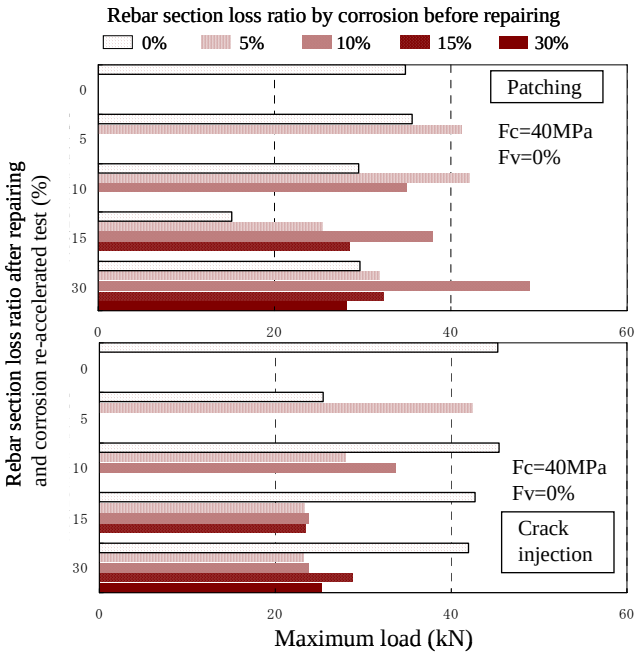

Figure 8. Maximum loads recovering ratio on repaired specimens and specimens subjected to accelerated rebar corrosion

Figure 6 shows the results of three-point loading tests on specimens with different degrees of deterioration before repair. The CMOD of normal strength specimens with no fibers increases as the section loss ratio increases under the same loads, presumably due to the losses in the adhesion of rebars. No clear changes related to the section loss ratio are ob-

served in high strength specimens with no fibers, presumably because the high strength of concrete prevents the adhesion of rebars from decreasing even under the corrosion-induced expansive pressure. In regard to specimens containing fibers, no marked increase in the displacement is observed with a section loss ratio of up to 15%, though the displacement is significant with a section loss ratio of 30%. Fibers are therefore expected to produce an effect of resisting the corrosion-induced expansive pressure.

Figure 7 and 8 shows the maximum loads and maximum road recovering ratio during three-point loading tests on repaired specimens and specimens subjected to accelerated rebar corrosion to the specified degrees after repair. When repaired by patching, the strength of repaired specimens with no corrosion is lower than unrepaired specimens with no corrosion. The strength of specimens with a higher degree of corrosion after repair is lower. When repaired by crack injection, the strength of specimens with a low degree of corrosion is higher than those repaired by patching, and the strength loss due to re-deterioration is also smaller than those repaired by patching. This can be attributed to increases in the strength of cover concrete impregnated with the injection resin. The strength after repair tends to decrease as the degree of corrosion before repair increases and as the degree of corrosion after repair increases, regardless of the repair method.

4 CONCLUSIONS

Conclusions of this study are as follows.

A method of analyzing the relationship between crack width and corrosion loss of reinforcement based on fracture mechanics was presented. By incorporating creep deformation near reinforcement, the analysis results agreed relatively well with the test results. A diagram for estimating the section loss ratio of internal reinforcement from the surface crack width was also presented.

The strength of cover concrete evaluated by three-point loading testing decreases as the section loss ratio of reinforcement increases, presumably due to reductions in the adhesion of reinforcement as corrosion develops. Increased strength of concrete and inclusion of fibers are effective measures against losses in the evaluated strength of cover concrete associated with reinforcement corrosion. When the degree of reinforcement corrosion is low, crack injection is more effective than patching in restoring the losses in the evaluated strength of cover concrete. Both patching and crack injection do not significantly contribute to the restoration of the evaluated strength losses of cover concrete. These are therefore considered to be of significance in inhibiting reinforcement corrosion.

5 APPENDIX

$$K_I = \frac{2f}{\sqrt{2d}} G(a,c,d) \tag{A.1}$$

$$G(a,c,d) = \left[1 + 0.297 \sqrt{1 - \left(\frac{c}{a}\right)^2} \left(1 - \cos\frac{\pi a}{2d} \right) \right] F(a,c,d) \tag{A.2}$$

$$K_I = \frac{2f}{\sqrt{\pi a}} G\left(a,c,d\right) \tag{A.3}$$

$$G(a,c,d) = \frac{G'(a,c,d)}{(1-A)^{3/2}\sqrt{1-B^2}}; \quad (A = a/d, B = c/a) \tag{A.4}$$

$$G'(a,c,d) = g_1(A) + g_2(A)\cdot B + g_3(A)\cdot B^2 + g_4(A)\cdot B^3$$

$$g_1(A) = 0.46 + 3.06A + 0.84(1-A)^5 + 0.66A^2(1-A)^2$$

$$g_2(A) = -3.52A^2$$

$$g_3(A) = 6.17 - 28.22A + 34.54A^2 - 14.39A^3 - (1-A)^{1.5}$$

$$-5.88(1-A)^5 - 2.64A^2(1-A)^2$$

$$g_4(A) = -6.63 + 25.16A - 31.04A^2 + 14.41A^3 + 2(1-A)^{1.5}$$

$$+5.04(1-A)^5 + 1.98A^2(1-A)^2$$

ACKNOWREDGEMENT

This study was conducted as a part of the 21st Century COE Program for Tokyo Metropolitan University, “Development of Technology for Activation and Renewal of building stocks in Megalopolis,” and as a part of the Ministry of Education, Science, Sports and Culture, Grant-in-Aid for scientific Research (B).

REFERENCES

Tada H, Paris PC, Irwin GR. 1985. The stress analysis of crack handbook, Second Edition. Paris Productions Incorporated.

Kitsutaka Y. 1997. Fracture parameters by poly-linear tension softening analysis. *Journal of Engineering Mechanics, ASCE* 123(5): 444-450.

Nakamura, N. & Kitsutaka, Y. 1998. Crack opening of high-strength concrete surface due to corrosion of reinforcing bar. *Proceedings of Japan Concrete Institute* 20(2): 871-876.